

A Prototype of an Integrated Pyranometer for Measuring Multi-Parameters

Faiz Syazwan Abdul Aziz¹ and Shahril Irwan Sulaiman²

Faculty of Electrical Engineering,
Universiti Teknologi MARA, 40450 Shah Alam, Selangor,
Malaysia

¹faizbopen@gmail.com ²shahril_irwan2004@yahoo.com

Hedzlin Zainuddin

Faculty of Applied Sciences
Universiti Teknologi MARA, 40450 Shah Alam, Selangor,
Malaysia

hedzlinzainuddin@yahoo.com

Abstract—This paper presents a handheld pyranometer which was integrated with temperature sensor modules. The pyranometer employs a reference solar cell which was calibrated to measure the solar irradiance. Besides the pyranometer, two temperature sensor modules were introduced to measure the ambient temperature and the photovoltaic module temperature. All measurements from the pyranometer and temperature sensors were controlled by a microcontroller PIC16F877A which later provided programming strategy in C language. The programming strategy was designed based on the calibrated solar cell and the temperature sensor modules while the measured values were displayed on an LCD display. The results showed that the prototype integrated pyranometer had relatively similar measured values when compared to a commercial pyranometer and a commercial temperature measuring tool.

Keywords—pyranometer; solar irradiance; ambient temperature; module temperature; photovoltaic

I. INTRODUCTION

The global depletion of fossil fuels has led to the growth of alternative energy resources such as renewable energy. One of the type of renewable energy is solar energy [1]. The solar energy utilizes photovoltaic (PV) modules to convert sunlight into electricity. Nevertheless, the performance of these PV modules is heavily dependent on the solar irradiance, ambient temperature and module temperature [2, 3]. The solar irradiance represents the intensity of sunlight whereas the ambient temperature and module temperature are related to surrounding air temperature and solar cell temperature respectively. Higher solar irradiance will lead to higher output current and therefore higher power output from a PV module [4]. On the other hand, the voltage of a PV module may decrease with the increase of ambient temperature and module temperature [5]. Unfortunately, these parameters are not fixed with respect to time as they depend severely on the weather conditions [6]. As a result, various measurement tools have been developed to instantaneously quantify these parameters.

The most important parameter in quantifying the input to PV module is the solar irradiance which represents a measure of incident solar radiation which falls on an area of a surface. The unit of solar irradiance is Watts per square meter (W/m²)

[7]. The solar irradiance is usually measured using a device known as pyranometer [8]. However, many modern pyranometers are dedicated to measure solar irradiance only, thus causing the function of the device to be limited although the ambient temperature and module temperature also play an important role in determining the PV module output.

Due to this limitation, an integrated pyranometer which is capable of measuring solar irradiance, ambient temperature and PV module temperature simultaneously is presented in this paper. This integrated pyranometer is expected to facilitate simultaneous measurement of the three parameters which are essential during an investigation of PV module performance.

II. METHODOLOGY

The development of the integrated pyranometer involved five major stages, namely the solar cell calibration, the temperature sensor selection, hardware development, PIC algorithm development as well as the performance analysis and evaluation.

A. Calibration of Solar Cell

In this study, a polycrystalline solar cell (6V/100mA) connected in parallel to a 100Ω resistor (100Ω) was used to calibrate the value of the solar irradiance. This solar cell was supposed to feed the resistor with current and voltage at a particular solar irradiance and ambient temperature. Firstly, the power generated by the solar cell at a specific solar irradiance, P_{CELL} can be estimated using

$$P_{CELL} = P_R \times \eta_{WIRE} \quad (1)$$

where P_R is the power dissipated in the resistor and η_{WIRE} is the wire efficiency which indicates the wire loss. Assuming the loss is too small, then

$$I_{CELL} = I_R \quad (2)$$

where I_{CELL} is the output current from the solar cell and I_R is the current flow through the resistor. This leads to

$$I_{CELL} = \frac{V_R}{R} \quad (3)$$

This work was supported in part by the Excellence Fund, Universiti Teknologi MARA, Malaysia (Ref: 600-RMI//DANA 5/3/Dst (283/2009)).

where V_R is the voltage across the resistor with a value R . I_{CELL} is therefore directly proportional to V_R and V_R is consequently is directly proportional to solar irradiance. The solar irradiance and V_R were simultaneously measured at different solar irradiance using a commercial pyranometer. The resulting relationship between solar irradiance and V_R is illustrated in Fig. 1. The linear regression shows that the measured solar irradiance, G can be represented as

$$G = 139.71V_R \tag{4}$$

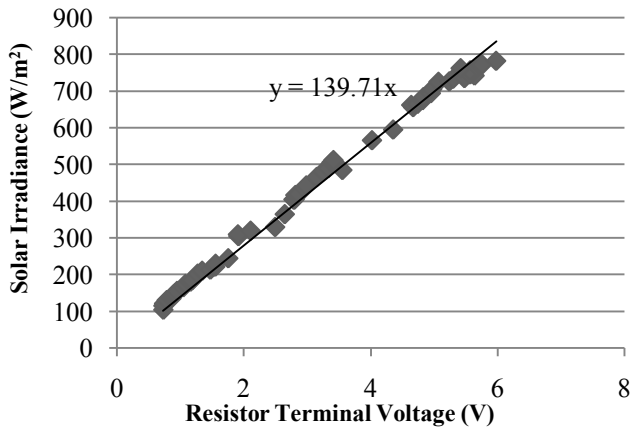


Fig. 1. Calibration of solar cell using solar irradiance and terminal voltage of resistor.

The solar cell acts as a reference cell for measuring solar irradiance. An investigation of the relationship between the short circuit current of the solar cell, I_{sc} and the corresponding solar irradiance was performed to evaluate the functionality of the solar cell for measuring solar irradiance.

B. Temperature Sensor Selection

After calibrating the solar cell, the temperature sensors were selected for measuring the ambient temperature and the PV module temperature. In this study, the LM35 Precision Centigrade Temperature Sensor was selected for measuring the ambient temperature while the DS18B20 Programmable Resolution 1-Wire Digital Thermometer was selected as the module temperature sensor. The LM35 sensor is a precision temperature sensor in which the output voltage is linearly proportional to the temperature in degree Celsius (Centigrade). On the other hand, the DS18B20 digital thermometer provides 9-bit to 12-bit Celsius temperature measurements and it communicates over a 1-Wire bus that requires only one data line for communication with a microcontroller.

C. Hardware Development

Once the solar cell and temperature sensors are ready to be integrated, the actual hardware was realized using microcontroller. In this project, the main components of the hardware were the solar cell, digital thermometer sensor, an ambient temperature sensor, Microcontroller and LCD for displaying the measured value. The integration of these components is shown in Fig. 2.

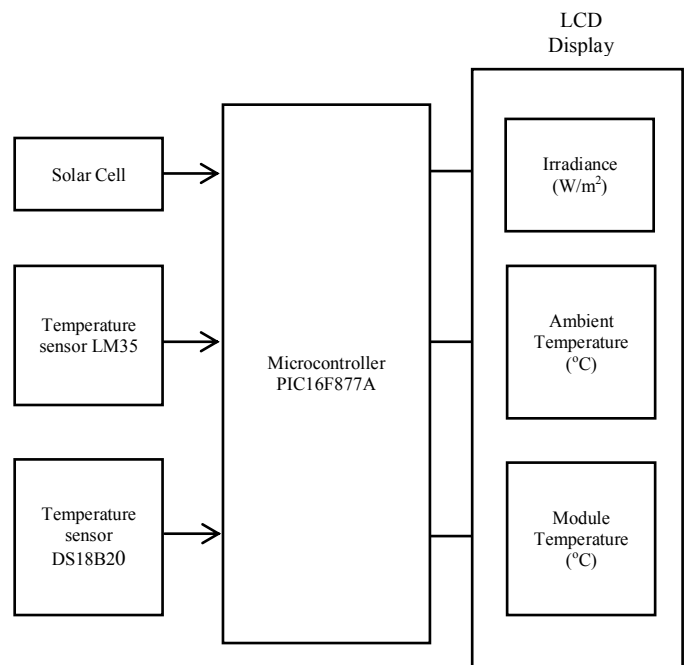


Fig. 2. System block diagram



Fig. 3. Prototype of the integrated pyranometer

In this study, PIC16F877A was chosen as the microcontroller for performing the necessary computation. It operates based on a program created using MPLab software. The measurement of solar irradiance was performed based on the measured terminal voltage of the resistor which was connected to the solar cell itself. Then, the terminal voltage of the resistor provided the analog voltage input for the analog-to-digital converter (ADC) port on the microcontroller. Subsequently, the ADC converted the analog voltages into digital forms. Similarly, the LM35 temperature sensor used to measure the ambient temperature was also connected to the ADC for transcription into digital form. However, the DS18B20 programmable resolution 1-wire digital thermometer was directly connected to the digital input port

on the microcontroller. All the inputs will be processed by the microcontroller and the measured solar irradiance, ambient temperature and module temperature will be displayed on an LCD. The final hardware realization is shown in Fig. 3.

D. PIC Algorithm Development

At this stage, the results from solar cell calibration were used to develop the PIC algorithm which was later programmed into PIC16F877A. The PIC algorithm was written using MPLAB software and the implementation is illustrated in Fig. 4. The program begins with the initialization of the input port for sensors and buttons, and output port for LCD. Then, there will be a display interface after the initialization process. Next, the program will check whether a button was pressed. Subsequently, the channel or input port is selected before passing input signal from the button to ADC port or digital input/output port. Finally, the measured value is processed and displayed on the LCD.

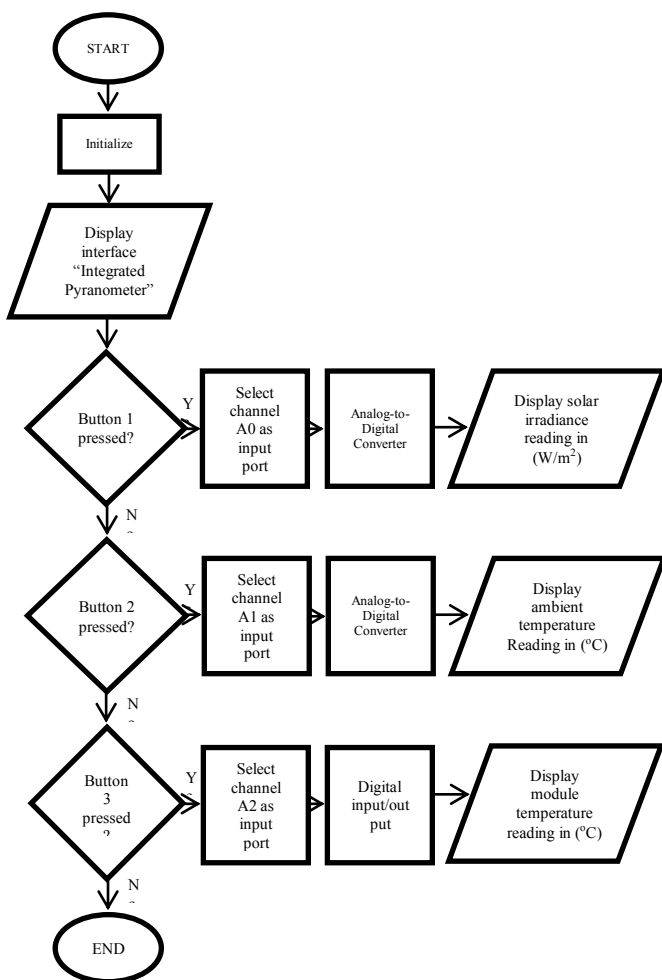


Fig. 4. PIC Algorithm Flow Chart

E. Performance Analysis and Evaluation

Upon completion of the prototype and PIC algorithm development, the performance of the integrated pyranometer

was evaluated. A field-test for solar irradiance measurement was performed using the integrated pyranometer and also an existing non-integrated commercial pyranometer (handheld pyranometer type 105hp by SolData Instruments) at different levels of solar irradiance. The output of these pyranometers was then compared for evaluation. Two performance indicators were chosen to quantify the performance of the newly developed integrated pyranometer, i.e. the percentage of error (PE) and the coefficient of determination (R^2).

1) Percent of Error

The difference between the measured value of a quantity x_0 and its actual value x is given by

$$\Delta x = |x_0 - x| \tag{5}$$

The percentage of error between the measured value of a quantity x_0 and its actual value x , given by

$$PE = \frac{|x_0 - x|}{x} \times 100\% \tag{6}$$

2) Coefficient of Determination

The R^2 is a measure of the goodness of fit of the model by calculating the proportion of measured variable values with actual variable values [9]. It can be computed using

$$R^2 = \frac{\sum(y_i - \bar{y})^2}{\sum(\hat{y}_i - \bar{y})^2} \tag{7}$$

where y_i is the observed value of the dependent variable while \bar{y} and \hat{y}_i are the mean and the fitted value respectively.

After that, the performance of the integrated pyranometer in ambient temperature measurement was evaluated by comparing the measured value with the measured value of the MiniTemp (Raytek) at different temperatures.

Besides that, the performance of the PV module temperature measurement was evaluating by benchmarking the value with the value produced by MiniTemp (Raytek) at different temperatures.

III. RESULTS AND DISCUSSION

Firstly, a field test was performed to compare the measured values of the prototype integrated pyranometer with those obtained using the commercial handheld pyranometer. However, the investigation of proportionality of the short circuit current of solar cell to solar irradiance had been initially conducted to evaluate the suitability of the solar cell for measuring solar irradiance. The relationship between the short circuit current of the solar cell with the corresponding irradiance is shown in Fig. 5. The coefficient of determination of the linear regression was 0.9654 which is very close to unity. Therefore, the solar irradiance was found to be almost linearly dependent with the short circuit current of the solar cell. In short, the solar cell is suitable for acting as a reference cell to measure solar irradiance.

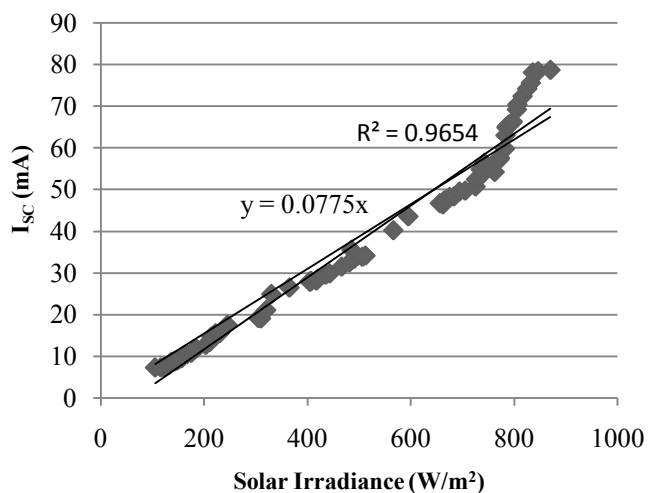


Fig. 5. Relationship between I_{sc} and solar irradiance

TABLE I
PERFORMANCE OF SOLAR IRRADIANCE MEASUREMENT

Type	Integrated Pyranometer	Handheld Pyranometer Type 105hp (SolData Instruments)	Percentage of Error (PE), in %
Solar Irradiance (W/m ²)	125	133	-6.01
	252	277	-9.03
	358	370	-3.24
	410	436	-5.96
	528	513	+2.92
	612	633	-3.32
	682	725	-5.93
	758	805	-5.84

Besides that, the performance of the prototype integrated pyranometer was benchmarked with the commercial pyranometer in measuring the solar irradiance. The resulting error measurement of solar irradiance is tabulated in Table I. Based on the arbitrary solar irradiance, the prototype integrated pyranometer showed promising results by producing measured solar irradiance value with errors between -6.01% to +2.92%. Thus, the results from the prototype integrated pyranometer are comparable with the results from the commercial pyranometer.

Later, the solar irradiance measurement was repeated using both pyranometers. The relationship between the measured values of the prototype integrated pyranometer and the commercial pyranometer is illustrated in Fig. 6. The linear regression shows that the prototype integrated pyranometer presented almost similar measured values as the commercial pyranometer with R^2 value of 0.9921.

Apart from the solar irradiance, the performance of ambient and PV module temperature measurements is shown

in Table 2. The ambient temperature measurement shows that the prototype integrated pyranometer had produced measurements with errors ranging from -2.86% to +2.70%. Thus, the difference between the measured temperature values from the prototype integrated pyranometer with those obtained using the MiniTemp (by Raytek) is relatively low. On the other hand, the results of the PV module temperature measurement in Table 3 show that the prototype integrated pyranometer had produced measurements with errors ranging from -2.22% to +2.13%. Therefore, the difference between the measured temperature values from the prototype integrated pyranometer with those obtained using the MiniTemp (by Raytek) was found to be low.

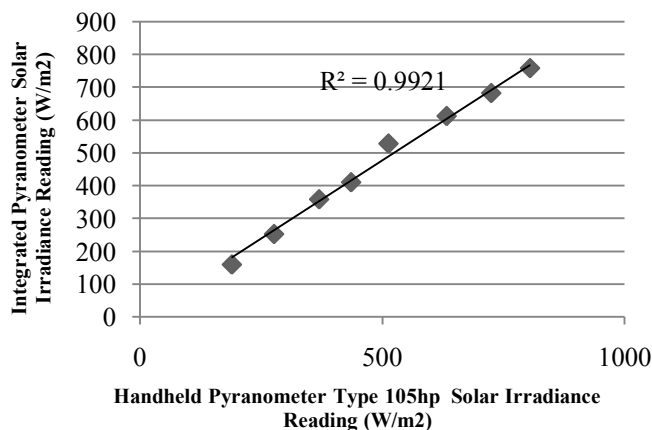


Fig. 6. Solar irradiance values measured using both pyranometers

TABLE II
PERFORMANCE OF AMBIENT TEMPERATURE MEASUREMENT

Type	Integrated Pyranometer	MiniTemp (Raytek)	Percentage of Error (PE), in %
Ambient Temperature (°C)	34	34	0.00
	34	34	0.00
	34	35	-2.86
	35	35	0.00
	35	36	-2.78
	36	37	-2.70
	37	37	0.00
	38	37	+2.70

TABLE III
PERFORMANCE OF PV MODULE TEMPERATURE MEASUREMENT

Type	Integrated Pyranometer	MiniTemp (Raytek)	Percentage of Error (PE), in %
Module Temperature (°C)	35	35	0.00
	42	42	0.00
	43	43	0.00
	44	45	-2.22
	46	47	-2.13
	48	48	0.00
	48	47	+2.13
	49	49	0.00

IV. CONCLUSION

A prototype integrated pyranometer has been designed and developed for measuring the solar irradiance, ambient temperature and PV module temperature simultaneously. When compared with a commercial pyranometer, the difference between the measured values of solar irradiance is relatively low. Similarly, when measuring the ambient temperature and PV module temperature, the difference between the measured values of the prototype integrated pyranometer and those obtained using a commercial temperature measuring tool is also low. Therefore, the developed prototype integrated pyranometer is expected to be useful for PV module performance evaluation as it is capable of measuring three different parameters at the same time.

ACKNOWLEDGMENT

The author would like to thank Green Energy Research Centre (GERC), Faculty of Electrical Engineering, Universiti Teknologi MARA Shah Alam for providing the facilities required for the work.

REFERENCES

[1] W. M. W. Mariam and S. Husni, "Influence of Malaysian climate on the efficiency of polycrystalline solar cells," in *2006. PCon '06. IEEE International Power and Energy Conference*, 2006, pp. 54-57.

[2] D. M. Riley and G. K. Venayagamoorthy, "Comparison of a recurrent neural network PV system model with a traditional component-based PV system model," in *37th IEEE Photovoltaic Specialists Conference (PVSC)*, 2011, pp. 2426-2431.

[3] D. M. Riley and G. K. Venayagamoorthy, "Characterization and modeling of a grid-connected photovoltaic system using a recurrent neural network," in *The 2011 International Joint Conference Neural Networks (IJCNN)*, 2011, pp. 1761-1766.

[4] S. Shaari, A. M. Omar, A. H. Haris, and S. I. Sulaiman, *Solar Photovoltaic Power: Fundamentals*. Putrajaya: Ministry of Energy, Green Technology and Water, 2010.

[5] E. Skoplaki and J. A. Palyvos, "Operating temperature of photovoltaic modules: A survey of pertinent correlations," *Renewable Energy*, vol. 34, pp. 23-29, January 2009.

[6] J. M. Gomes, P. M. Ferreira, and A. E. Ruano, "Implementation of an intelligent sensor for measurement and prediction of solar radiation and atmospheric temperature," in *IEEE 7th International Symposium Intelligent Signal Processing (WISP)*, 2011, pp. 1-6.

[7] P. Attaviriyapap, K. Tokuhara, N. Itaya, M. Marmiroli, Y. Tsukamoto, and Y. Kojima, "Estimation of photovoltaic power generation output based on solar irradiation and frequency classification," in *IEEE PES Innovative Smart Grid Technologies Asia (ISGT)*, 2011, pp. 1-7.

[8] M. A. Martinez, J. M. Andujar, and J. M. Enrique, "A new and inexpensive pyranometer for the visible spectral range," *Sensors*, vol. 9, pp. 4615-4634, June 2009.

[9] S. I. Sulaiman, T. K. A. Rahman, I. Musirin, and S. Shaari, "Fast evolutionary programming-based hybrid multi-layer feedforward neural network for predicting grid-connected photovoltaic system output," in *International Colloquium on Signal Processing & Its Applications (CSPA2012)*, Melaka, 2012, pp. 32-35.